IEEE Access
Multidisciplinary | Rapid Review | Open Access Journal

Received April 1, 2021, accepted April 12, 2021, date of publication April 21, 2021, date of current version April 29, 2021.

Digital Object Identifier 10.1109/ACCESS.2021.3074579

Tri-Objective Optimal PMU Placement Including Accurate State Estimation: The Case of Distribution Systems

RICCARDO ANDREONI, DAVID MACII, (Senior Member, IEEE), MATTEO BRUNELLI, AND DARIO PETRI, (Fellow, IEEE)
Department of Industrial Engineering, University of Trento, 38123 Trento, Italy

Corresponding author: David Macii (david.macii@unitn.it)

This work was supported in part by the Project "Dipartimenti di eccellenza-2018–2022" funded by the Italian Ministry for University and Research.

ABSTRACT This paper presents a tri-objective Optimal Phasor Measurement Units (PMUs) Placement (OPP) strategy that is focused on the minimization of i) the total number of PMU channels, ii) the maximum state estimation uncertainty based only on high-rate PMU data and iii) the sensitivity of state estimation to line parameter tolerances. The proposed formulation keeps into account system observability with and without contingencies due to single-line and PMU faults. Also, it includes the effect of possible zero-injection buses and a-priori constraints on both the number of PMU channels and the type of PMU measurements performed at each bus. Due to the nonlinear combinatorial nature of the proposed OPP problem, this is solved through a custom implementation of the nondominated sorting genetic algorithm II (NSGA-II). The analysis of the proposed OPP strategy is focused on distribution systems. The placement results obtained using four test systems of different size show that increasing the number of buses instrumented with PMUs and/or the number of PMU channels beyond given thresholds just leads to larger costs with negligible further reductions in both state estimation uncertainty and sensitivity to line parameters tolerances. Moreover, if PMUs with just two three-phase channels are used, we can avoid instrumenting between 30% and 40% of buses with a minor impact on state estimation performance even in the case of contingencies. This percentage can be slightly increased if multi-channel PMUs are used. However, this choice generally is not profitable.

INDEX TERMS Distribution system state estimation, multi-objective optimization, optimal PMU placement, phasor measurement unit (PMU), power systems monitoring.

I. INTRODUCTION

Phasor Measurement Units (PMUs) are measuring devices conceived to collect estimates of magnitude, phase, frequency and rate of change of frequency of current or voltage AC waveforms synchronized to the Coordinated Universal Time (UTC) with reporting rates in the order of tens of Hz [1]–[3]. The PMUs typically deployed in power transmission systems since the '90s have played a key role for protection purposes, namely to detect faults or other impending critical operating conditions timely. Unfortunately, due to the high equipment cost and the huge amount of data that is supposed to be collected by the so-called Phasor Data Concentrators, the deployment of PMUs is notoriously a delicate problem, which is further complicated by the need to ensure adequate system observability.

The associate editor coordinating the review of this manuscript and approving it for publication was Lin Zhang.

While the vast majority of research works on Optimal PMU Placement (OPP) relies on a cumulative single objective function and is focused on transmission system deployment, the main contribution of this paper is threefold, i.e.

- the definition of a multi-objective strategy where contrasting goals are considered;
- the inclusion of constraints not only for observability under contingencies, but also on the number and the type of PMU measurements that can be performed at each bus (this aspect is disregarded in many papers on OPP);
- the focus on distribution systems, which is an emerging field of application for PMUs.

The objective functions considered in this paper are: the total number of PMU channels (which is one of the factor that most strongly affects the growth of instrumental cost), the maximum state estimation uncertainty (assuming that only high-rate PMU measurements are used) and the

maximum sensitivity of state estimation uncertainty to line parameter tolerances. Such objective functions are optimized under different conditions, ranging from basic system observability to the ability to withstand critical contingencies such as single-line outages or the loss of data from a PMU. Given the tri-objective nonlinear formulation of the problem at hand, a custom implementation of the Nondominated Sorting Genetic Algorithm II (NSGA-II) is used to find the PMU sites minimizing at least one objective function [4], namely the Pareto frontier of the set of possible solutions [5].

Even though the proposed formulation can be applied to any kind of power system, the results reported in this paper refer specifically to the case of distribution systems because nowadays the so-called distribution-level PMUs are regarded as essential for real-time smart-grid and micro-grid future flexible operations under changeable conditions of load and generation [6]–[8]. Moreover, the chosen OPP strategy is more suitable to the case of distribution systems due to the large potential number of buses and quantities to be measured, the greater uncertainty affecting grid line parameters and, last but not least, the need to estimate state variables (e.g., the bus voltage phasors) that differ from one another much less than at the transmission level.

The rest of the paper is structured as follows. Section II highlights more in detail the specific and novel features of the proposed approach with respect to other OPP solutions. In Section III the tri-objective OPP problem is formalized and, after a general overview, the individual objective functions are defined and justified. Section IV provides a short, but exhaustive explanation of how the NSGA-II is implemented and initialized in the case at hand. In Section V, the results of the proposed OPP strategy using four test distribution systems of increasing size are reported considering different constraints. Finally, after a cost analysis example in Section VI, the main conclusions are drawn in Section VII.

II. RELATED WORK

As outlined in the Introduction, most of the OPP problem formulations rely on a single objective function. Their main goal is to minimize PMU deployment cost (or sometimes simply the total number of PMUs), while preserving full system observability (namely the ability to estimate the state of the whole grid at a given time), although some studies on OPP in the case of incomplete observability were also conducted, e.g. in [9].

Since both the total PMU deployment cost and the topological observability generally depend linearly on the number of PMUs, initially the OPP problem was solved by using standard integer (usually binary) linear programming optimization methods [10]. For instance, an OPP Integer Linear Programming (ILP) formulation was proposed by Xu and Abur [11]. An alternative approach was proposed in [12] to minimize the number of PMUs needed to attain complete power system observability, while improving state estimation robustness through redundant critical measurements. A similar distinction between critical and redundant measurements was proposed in [13] to detect bad data in state estimation.

Over the years, the basic OPP problem has become more and more involved due to the inclusion of increasingly sophisticated and heterogeneous operating conditions and constraints. These may include (but are not limited to):

- the use of conventional measurements [14]–[16], power flow measurements [17], or smart meter data supporting system observability [18];
- information provided by load loss and relaying [19], or zero-injection buses [20], [21];
- contingencies due to line outages and/or PMU losses [22]–[26];
- system component reliability data to reduce the redundancy requirements for observability in the case of contingencies [27];
- communication constraints [28], or limits in the number of PMU channels [29]–[32].

The finite number of PMU channels (a constraint that was often disregarded in past studies on OPP) can greatly affect the results and the impact of PMU placement with and without contingencies [33]. Indeed, if the number of channels of a PMU is smaller than the number of lines connected to the bus where the PMU is installed, a combinatorial amount of possible line current phasor measurements exists [31]. Such configurations increase the number of conditions to be included in the observability constraint [32]. Thus, including such conditions in the problem formulation leads to a fast growth in the number of rows of the connectivity matrix used to implement the observability constraint. This situation can be very hard to manage in distribution systems that usually consist of a large number of nodes. For this reason, in this paper the lines that are not observed directly by a PMU due to the limited number of channels are decided a priori.

Nowadays, the OPP problem formulation includes most of the conditions listed above within a unique framework. Moreover, also the objective function has gradually become increasingly complex and it is given by a linear or quadratic combination of multiple terms. However, this function generally takes into account only economic and observability aspects, whereas the impact of PMUs performance is typically disregarded at all. Just to provide some examples, Chakrabarti *et al.* [34] proposed an integer quadratic programming OPP formulation, in which the objective function consists of two terms: one representing the redundancy level of PMU placement and another one quantifying the overall PMU installation costs. The single-objective cost function adopted in [35] aims at minimizing the number of PMUs deployed in the system, while maximizing network observability and minimizing the sensitivity to grid parameters. The objective function defined in [36] includes not only the total deployment costs, but also additional terms keeping into account the cost of redundancies to enhance system observability and the cost of network unobservability both in normal operating conditions and under contingencies.

The main downside of single-objective optimization is the need to aggregate different quantities into a scalar cost function so that a single solution is obtained. Such an aggregation is usually performed by weighing the objectives considered in the problem. However, the outcome of this approach strongly relies on the chosen weights, which may eventually lead to lack of stability and/or diversity [37].

On the other hand,''the generalization of the OPP problem considering multiple objectives including not only installation cost, but also redundancy, performance, and other planning constraints'' is currently regarded as one of the main future research direction in this field [38]. At the moment, just a limited number of research works on OPP are based on a multi-objective formulation, most of them including two objectives. In [39] and [37], the PMU placement is driven by both the minimization of the number of PMUs and the maximization of measurement redundancy, which are indeed contrasting goals. However, again state estimation uncertainty and sensitivity to line tolerances are not taken into account, as instead it is done in our work.

The general idea of using such objective functions is quite uncommon in the panorama of OPP solutions. Nevertheless, at the distribution level this is justified by i) the need for superior performance since the state variables of monitored systems are characterized by small amplitude and angle differences [40] and ii) the larger uncertainty affecting line parameters compared to the case of transmission systems. The idea of optimizing both accuracy and robustness is also the basis of the placement technique described in [41]. However, that solution is totally different from the approach proposed in this paper because i) it is focused on meter instead of PMU placement and ii) it relies on a two-step optimization procedure rather than a multi-objective one. In fact, while the two-step optimization algorithms are likely to find solutions that are just locally optimal, a proper multi-objective optimization can provide deeper insights about benefits, drawbacks and possible trade-offs between different nondominated solutions. To the best of Authors' knowledge, the only example of a tri-objective approach for OPP is described in [42], which, similarly to our work, relies on the idea of finding the best trade-off between PMU deployment cost and power system monitoring robustness. However, the objective functions in [42] (i.e., the best assessment of small signal stability based on PMU data; the maximization of the probability of system observability if anomalous events occur and the minimization of PMUs total cost) are inherently different and hardly comparable with the approach adopted in this paper. In fact, as stated in the Introduction, the proposed OPP strategy is specifically conceived to minimize state estimation uncertainty and sensitivity to line tolerances in grids that exhibit very small state variables variations in both magnitude and phase.

As far as the OPP problem solver is concerned, a comprehensive review of possible techniques is presented in [43]. However, even though a variety of heuristic algorithms exists to find satisfactory sub-optimal solutions within a reasonable time (e.g., tabu search, simulated annealing, particle swarm optimization, spanning-tree search, genetic algorithms, and binary harmony search [44]), in this paper a custom version of the NSGA-II algorithm is implemented. The use of a genetic algorithm for multi-objective OPP is in line with the approaches adopted in other papers [37], [39]. Among them, NSGA-II is particularly versatile and suitable to find the Pareto frontier with high accuracy, as confirmed by a large number of tests on benchmark problems [45], and by the fact that the same algorithm has been already used for OPP, although the problem formulation in [42] is completely different. Two further key factors that make the NSGA-II approach particularly suitable in the case at hand are: the easiness in generating a good initial population and the use of penalties to remove infeasible solutions.

III. PROBLEM FORMULATION

Given a grid consisting of N buses and L lines, let $\mathbf{x} \in \mathbb{X} = \{0,1\}^N$ be a binary vector whose ith element x_i is set to 1 or 0 depending on whether a PMU is deployed to the ith bus or not. In general, if the number of PMU channels is large enough to measure the current phasors of some of the lines connecting a given bus with the adjacent ones, a PMU can potentially observe not only the state variables of the bus where the PMU is deployed directly, but also those of all the buses that are connected through the monitored lines. However, if there are Zero-Injection (ZI) buses with a zero-injection observation depth smaller than or equal to 1 (as generally occurs at the distribution level), an auxiliary binary decision vector $\mathbf{u}$ can be introduced to relax system observability [21]. In particular, the ith element u_i of $\mathbf{u}$ can be set to 1 if bus i is a ZI bus and, for a given placement configuration $\mathbf{x}$, all nodes adjacent to bus i (except at most one) are observed directly or indirectly.

On the basis of the vector variables defined above, if function $\mathsf{C}(\mathbf{x})$ represents the total number of PMU channels available for grid monitoring based on the placement given by $\mathbf{x}$, $\mathsf{U}(\mathbf{x})$ is the corresponding maximum state estimation uncertainty and $\mathsf{S}(\mathbf{x})$ is the maximum sensitivity to grid parameter tolerances (further details on the definition of such objective functions are reported in Subsections III-A-III-C), the proposed tri-objective OPP problem can be formalized as follows;

$$\min_{\mathbf{x}\in\mathbb{X}} (\mathsf{C}(\mathbf{x}), \mathsf{U}(\mathbf{x}), \mathsf{S}(\mathbf{x})) \tag{1}$$

subject to two sets of constraints, i.e. those ensuring full system observability using only PMU measurements and those that keep into account the PMU measurements that can be actually performed at each bus if the number of PMU channels is limited. Both constraints are formalized below.

1) System observability based only on PMU measurements and ZI buses can be guaranteed without contingencies through the following inequality [11], i.e.

$$\mathbf{A}(\mathbf{x}+\mathbf{u}) \geq \mathbf{1} \tag{1a}$$

where $\mathbf{1}$ is an all-one vector and $\mathbf{A}$ is the $N \times N$ symmetric binary connectivity matrix of the undirected graph modeling the considered grid (i.e., $a_{ij} = 1$ if either $i = j$ or buses i and j are directly connected, and $a_{ij} = 0$ otherwise). However, if one PMU is lost or a single line fault occurs, a stricter observability constraint than (1a) is needed, i.e.

$$\begin{bmatrix} \tilde{\mathbf{A}}^1 \\ \vdots \\ \tilde{\mathbf{A}}^N \end{bmatrix} (\mathbf{x} + \mathbf{u}) \geq \mathbf{1} \text{ and } \begin{bmatrix} \hat{\mathbf{A}}^1 \\ \vdots \\ \hat{\mathbf{A}}^L \end{bmatrix} (\mathbf{x} + \mathbf{u}) \geq \mathbf{1}, \quad (1b)$$

where matrix $\tilde{\mathbf{A}}^b$ for $b = 1, \ldots, N$ is obtained by replacing the bth column of $\mathbf{A}$ with an all-zero vector. Similarly, matrix $\hat{\mathbf{A}}^l$ for $l = 1, \ldots, L$ is obtained by resetting the elements of $\mathbf{A}$ indexed by (i, j) and (j, i), namely the elements corresponding to buses i and j that are connected through the lth line. The former inequality ensures observability even if the measurements from the PMU installed at a generic bus b (for $b = 1, \ldots, N$) are lost. The latter one mitigates the effect of a fault occurring in any one of the L lines.

2) The PMU measurements that can be performed at the ith bus depend on both the type of measurement and the maximum number n_{c_i} of available PMU channels. It is worth reminding that many papers on OPP disregard the number of PMU channels. In fact, not all current phasors are actually monitored and used for state estimation. In this paper instead, this inherent technology-related constraint is taken into consideration. Assuming that one channel of each PMU is used for bus voltage phasor measurement (namely to observe the state variable directly), while the remaining $n_{c_i} - 1$ are used for current phasor measurements, the constraint on the number of allowed measurements can be formalized as follows, i.e.,

$$\begin{bmatrix} \mathbf{I}_N & \mathbf{\Gamma} \end{bmatrix} \begin{bmatrix} \mathbf{x} \\ \mathbf{x} \end{bmatrix} \leq \mathbf{n_c} \quad (1c)$$

where $\mathbf{n_c}$ is the column vector including the maximum number of channels of all PMUs, $\mathbf{I}_N$ is the $N \times N$ identity matrix, and finally $\mathbf{\Gamma}$ is an $N \times N$ binary matrix defining the current phasor measurements that can be performed at every bus. In particular, the diagonal entries γ_{ii} of $\mathbf{\Gamma}$ for $i = 1, \ldots, N$ are set to 1 only if one channel of the PMU placed at bus i is used to measure the injection current phasor at that bus. Of course, the diagonal entries γ_{ii} corresponding to the ZI buses and the buses when no PMU is placed are null. Similarly, the nondiagonal elements γ_{ij} of $\mathbf{\Gamma}$ are set to 1 if the PMU placed at bus j is used to measure the phasor of the current flowing through the line connecting bus i with bus j. Note that matrix $\mathbf{\Gamma}$ is not required to be symmetric because, if a given line current phasor is monitored by a PMU at one end of the line, the measurement of the same current phasor at the other end of the line is not needed (i.e., if $\gamma_{ij} = 1$, then γ_{ji} can be set to 0), unless some redundancy is required. Observe also that if $\mathbf{\Gamma}$ coincides with the connectivity matrix and n_{c_i} is greater than or equal to the number of lines connected to bus i plus 2, constraint (1c) is always satisfied and therefore it can be omitted in OPP formulation.

A. OBJECTIVE 1: MINIMUM TOTAL NUMBER OF PMU CHANNELS

In most OPP problems, the cost function considered for PMU deployment is assumed to grow linearly with the number of measuring devices and often include multiple terms, e.g. the costs due to service disruption for PMU installation in the substations, the PMU hardware and labor costs, and variable costs depending on the number of channels [46]. Due to the large variability of such factors (as documented for instance in [47]), in Authors' opinion the use of a multi-parametric cost function including a variety of economic terms is quite questionable in the case at hand. In fact, the OPP results and the related conclusions could be highly dependent on the values of the chosen parameters, which in turn may strongly change as a function of both technology and market-related or context-specific aspects. Therefore, to keep the PMU placement strategy as general as possible, in the rest of this paper just the total number of PMU channels is considered as the first objective function for OPP. Indeed, this quantity not only grows with the number of deployed PMUs (which is the most basic cost function in OPP problems), but it also has a significant impact on equipment cost due to both the PMU device per se and the voltage and current measurement transducers connected to each channel. Thus, we have that

$$\mathsf{C}(\mathbf{x}) = \mathbf{c}^T \cdot \mathbf{x} \quad (2)$$

where $\mathbf{c} \leq \mathbf{n_c}$ is the column vector including the number of PMU channels available for both voltage and current measurements at all buses. Even if (2) cannot return a clear and complete cost evaluation of a given PMU placement, it is simple and general enough to allow a sensible, although approximate, economic comparison of different OPP solutions, as it will be shown in the case study reported in Section VI.

B. OBJECTIVE 2: PMU-BASED MINIMAX STATE ESTIMATION UNCERTAINTY

The objective function about state estimation uncertainty depends on both the selected state estimator and the parameter chosen "to characterize the dispersion of the values that could reasonably be attributed to the measurand" [48]. The weighted least squares estimator adopted in this paper relies on two assumptions, i.e.

1) only the information based on ZI buses and PMU data are used for state estimation;
2) the state variables as well as the voltage and current phasor measurements are transformed from polar to rectangular coordinates as in [49], [50].

The former assumption is motivated by the purpose of this study that intends to evaluate the potential impact of PMUs in

a futuristic scenario where the state of active distribution grids is estimated in real-time at a rate that could not be possible with traditional measurements [51]. Thus, even though traditional measurements and pseudo-measurements can certainly support observability and state estimation, they will not be considered in the following. In fact, system observability is provided by ZI buses and PMUs only. This assumption is indeed quite common in research works on OPP strategies.

The choice of using rectangular variables stems instead from the simple formalization of the linear system of equations used for state estimation [see expressions (3)-(6) in the following], with relevant benefits from the computational point of view [52].

Let $\mathbf{x} \in \mathbb{X}$ be the binary vector expressing the buses where the PMUs are placed. If M_V is the number of non-zero elements of $\mathbf{x}$, at least M_V bus voltage phasor measurement can be performed. Therefore, system state estimation relies on i) M_V bus voltage phasor measurement, ii) M_I current phasor measurements [depending on constraint (1c)], and M_z ZI current measurements (in fact, this number coincides with the number of ZI buses). Such $M = M_V + M_I + M_z \geq N$ measurement data (split into real and imaginary parts denoted with subscripts R and I, respectively) can be merged into a single $2M-$long vector $\mathbf{z} = [\mathbf{z}_{V_R}^T, \mathbf{z}_{V_I}^T, \mathbf{z}_{I_R}^T, \mathbf{z}_{I_I}^T, \mathbf{0}^T, \mathbf{0}^T]^T$. If also the state variables (namely the bus voltage phasors) are expressed into rectangular coordinates and are rearranged into a $2N-$long vector $\mathbf{v} = [\mathbf{v}_R^T, \mathbf{v}_I^T]^T$, the relationship between measurement data and state variables can be expressed by the following linear system of equations, i.e. [49], [50]

$$\mathbf{z} = \begin{bmatrix} \mathbf{z}_{V_R} \\ \mathbf{z}_{V_I} \\ \mathbf{z}_{I_R} \\ \mathbf{z}_{I_I} \\ \mathbf{0} \\ \mathbf{0} \end{bmatrix} = \mathbf{H}(\mathbf{x}) \begin{bmatrix} \mathbf{v}_R^T, \\ \mathbf{v}_I^T, \end{bmatrix} + \boldsymbol{\varepsilon} \tag{3}$$

where $\boldsymbol{\varepsilon} = [\boldsymbol{\varepsilon}_{V_R}^T, \boldsymbol{\varepsilon}_{V_I}^T, \boldsymbol{\varepsilon}_{I_R}^T, \boldsymbol{\varepsilon}_{I_I}^T, \boldsymbol{\varepsilon}_z^T, \boldsymbol{\varepsilon}_z^T]^T$ is the column vector including the random uncertainty contributions affecting different kind of measurements, and

$$\mathbf{H}(\mathbf{x}) = \begin{bmatrix} \tilde{\mathbf{I}}(\mathbf{x}) & \mathbf{0} \\ \mathbf{0} & \tilde{\mathbf{I}}(\mathbf{x}) \\ \mathbf{G}(\mathbf{x}) & -\mathbf{B}(\mathbf{x}) \\ \mathbf{B}(\mathbf{x}) & \mathbf{G}(\mathbf{x}) \\ \mathbf{G}_z & -\mathbf{B}_z \\ \mathbf{B}_z & \mathbf{G}_z \end{bmatrix} \tag{4}$$

is $2M \times 2N$ block matrix where

- the $M_V \times N$ matrix $\tilde{\mathbf{I}}(\mathbf{x})$ is obtained from the $N \times N$ identity matrix $\mathbf{I}_N$ by removing the $N - M_V$ rows corresponding to the elements of $\mathbf{x}$ equal to 0, namely the buses where no PMUs are placed. In practice, matrix $\tilde{\mathbf{I}}(\mathbf{x})$ identifies the voltage phasors that can observed directly.
- the $M_I \times N$ matrices

$$\mathbf{G}(\mathbf{x}) = \begin{bmatrix} \mathbf{G}_l(\mathbf{x}) \\ \mathbf{G}_b(\mathbf{x}) \end{bmatrix} \quad \text{and} \quad \mathbf{B}(\mathbf{x}) = \begin{bmatrix} \mathbf{B}_l(\mathbf{x}) \\ \mathbf{B}_b(\mathbf{x}) \end{bmatrix} \tag{5}$$

express the relationship between the current phasors actually measured by the PMUs placed as specified in vector $\mathbf{x}$ and the bus voltage phasors. In particular, the rows of submatrices $\mathbf{G}_l(\mathbf{x})$ and $\mathbf{G}_b(\mathbf{x})$ include just two non-zero elements with the same absolute value, but with opposite sign, i.e. the conductance and susceptance values, respectively, of the lines monitored by the deployed PMUs. Dually, submatrices $\mathbf{G}_b(\mathbf{x})$ and $\mathbf{B}_b(\mathbf{x})$ comprise the rows of the real and imaginary parts, respectively, of the grid admittance matrix corresponding to the buses whose injection current phasors (due only to loads in the case of purely passive systems) are measured by the available PMUs. The general expressions of the line admittances and the elements of the grid admittance matrix can be found for instance in [53].

- Finally, matrices $\mathbf{G}_z$ and $\mathbf{B}_z$ are also extracted from the grid admittance matrix, but they do not depend on the PMU placement in $\mathbf{x}$, as they include the rows of the conductance and susceptance values, respectively, of the elements corresponding to the ZI buses.

Assuming that the measurement uncertainty contributions $\boldsymbol{\varepsilon}$ in (3) are normally distributed with zero mean and covariance matrix $\mathbf{R} = \mathbb{E}\{\boldsymbol{\varepsilon}\boldsymbol{\varepsilon}^T\}$ (the expressions of the variances of voltage or current phasor measurements expressed into rectangular coordinates are reported in the Appendix), the best linear unbiased estimator of the system state is the weighted least-squares estimator given by [49], [50]

$$\hat{\mathbf{v}} = \mathbf{F}(\mathbf{x})\mathbf{z} = [\mathbf{H}^T(\mathbf{x})\mathbf{R}^{-1}\mathbf{H}(\mathbf{x})]^{-1}\mathbf{H}^T(\mathbf{x})\mathbf{R}^{-1}\mathbf{z}, \tag{6}$$

where symbol $\hat{\cdot}$ denotes an estimated quantity (i.e., the state vector in this case). Consider that, if all measurement uncertainty contributions are assumed to be uncorrelated, $\mathbf{R}$ is diagonal. Also, the elements associated with ZI current measurements should be null. However, they are replaced by very small (but non-zero) values (i.e., at least two orders of magnitude lower than the other nonzero elements of $\mathbf{R}$) to make matrix $\mathbf{R}$ invertible.

Let $\mathbf{e}_v^c = (\hat{\mathbf{v}}_R - \mathbf{v}_R) + j(\hat{\mathbf{v}}_I - \mathbf{v}_I)$ be the $N \times 1$ random complex error vector resulting from the zero-mean estimation errors of the real and imaginary parts of the state variables. Since $\Phi_v^c = \mathbb{E}\{\mathbf{e}_v^c \mathbf{e}_v^{cH}\}$ (with ^{H} denoting the Hermitian operator) is the covariance matrix of the complex state estimation errors, a possible scalar and conservative function expressing the state estimation uncertainty is

$$\mathsf{U}(\mathbf{x}) = \max\left\{\sqrt{|\mathrm{Eig}(\Phi_v^c)|}\right\} \tag{7}$$

where function $\mathrm{Eig}(\cdot)$ returns the eigenvalues of the argument matrix. The rationale for choosing (7) as the objective function for estimation uncertainty is that, from a geometrical standpoint, the maximum eigenvalue of Φ_v^c represents the radius of the hypersphere circumscribing the ellipsoidal uncertainty region around the estimated state [54].

C. OBJECTIVE 3: MINIMAX SENSITIVITY TO LINE PARAMETER TOLERANCES

No unique definition exists to express the sensitivity of system state estimation to the uncertainty affecting grid parameters. In this paper, the sensitivity function $\mathsf{S}(\mathbf{x})$ is defined as the maximum increment of the elements of the covariance matrix of state estimation errors due to unknown (but bounded) tolerances of line parameters for a given measurement configuration. If the elements of matrix $\mathbf{H}(\mathbf{x})$ defined in (4) are affected by uncertainty, then in the measurement model (3), $\mathbf{H}(\mathbf{x})$ has to be replaced by $\tilde{\mathbf{H}}(\mathbf{x}) = \mathbf{H}(\mathbf{x}) + \boldsymbol{\delta}\mathbf{H}(\mathbf{x})$ where

$$\boldsymbol{\delta}\mathbf{H}(\mathbf{x}) = \begin{bmatrix} \mathbf{0} & \mathbf{0} \\ \mathbf{0} & \mathbf{0} \\ \boldsymbol{\delta}\mathbf{G}(\mathbf{x}) & -\boldsymbol{\delta}\mathbf{B}(\mathbf{x}) \\ \boldsymbol{\delta}\mathbf{B}(\mathbf{x}) & \boldsymbol{\delta}\mathbf{G}(\mathbf{x}) \\ \boldsymbol{\delta}\mathbf{G}_z & -\boldsymbol{\delta}\mathbf{B}_z \\ \boldsymbol{\delta}\mathbf{B}_z & \boldsymbol{\delta}\mathbf{G}_z \end{bmatrix} \tag{8}$$

is the so-called perturbation matrix due to possible tolerances. Assuming that the estimation errors of the real and imaginary parts of the chosen state variables given by (6) are rearranged into the $2N \times 1$ vector $\mathbf{e}_v = [(\hat{\mathbf{v}}_R - \mathbf{v}_R)^T, \ (\hat{\mathbf{v}}_I - \mathbf{v}_I)^T]^T$, the covariance matrix of $\mathbf{e}_v$ can be expressed as [55]

$$\tilde{\Phi}_v = \mathbb{E}(\mathbf{e}_v \mathbf{e}_v^T) = \tilde{\mathbf{F}}(\mathbf{x})\mathbb{E}\{\boldsymbol{\varepsilon}\boldsymbol{\varepsilon}^T\}\tilde{\mathbf{F}}^T(\mathbf{x}) = \tilde{\mathbf{F}}(\mathbf{x})\mathbf{R}\tilde{\mathbf{F}}^T(\mathbf{x}) \tag{9}$$

where $\tilde{\mathbf{F}}(\mathbf{x}) = [\tilde{\mathbf{H}}^T(\mathbf{x})\mathbf{R}^{-1}\tilde{\mathbf{H}}(\mathbf{x})]^{-1}\tilde{\mathbf{H}}^T(\mathbf{x})\mathbf{R}^{-1}$. To evaluate the impact of line parameter tolerances on $\tilde{\Phi}_{\mathbf{v}}$ regardless of the uncertainty of the available measurements, the effect of tolerances and measurement uncertainty in (9) has to be decoupled. This result can be achieved if all measurements are uncorrelated, the relative standard uncertainty of all deployed PMUs is assumed to be the same and the PMU Total Vector Errors (TVEs) are evenly split between magnitude and phase contributions. In particular, if σ_r denotes the relative standard uncertainty common to all measurements, then matrix $\mathbf{R}$ can be rewritten as $\mathbf{R} = \sigma_r^2\tilde{\mathbf{R}}$. Therefore, recalling that $\tilde{\mathbf{R}}^{-1} = \tilde{\mathbf{R}}^{-1^T}$, after a few steps (9) can be rewritten as

$$\tilde{\Phi}_v = \tilde{\mathbf{S}}(\mathbf{x})\sigma_r^2 = [\tilde{\mathbf{H}}^T(\mathbf{x})\tilde{\mathbf{R}}^{-1}\tilde{\mathbf{H}}(\mathbf{x})]^{-1}\sigma_r^2 \tag{10}$$

where $\tilde{\mathbf{S}}(\mathbf{x})$ can be regarded as the sensitivity matrix, since its elements represent the rates of change of the entries of the covariance matrix of state estimation errors due just to the tolerance values. If the elements of (8) are assumed to be uniformly distributed around the respective nominal values within a given relative fraction $\pm\Delta$ of H_{ij} for $j = 1, \ldots, 2M$ and $i = 1, \ldots, 2N$, a possible scalar objective function expressing the maximum sensitivity to line parameter tolerances is

$$\mathsf{S}(\mathbf{x}) = \max_{i,j=1,\ldots,N} \left\{ \max_{\delta H_{ij} \in [-\Delta \cdot H_{ij}, \Delta \cdot H_{ij}]} \left\{ \tilde{S}_{ij} \right\} \right\}. \tag{11}$$

This function is in accordance with the definition provided at the beginning of this Section.

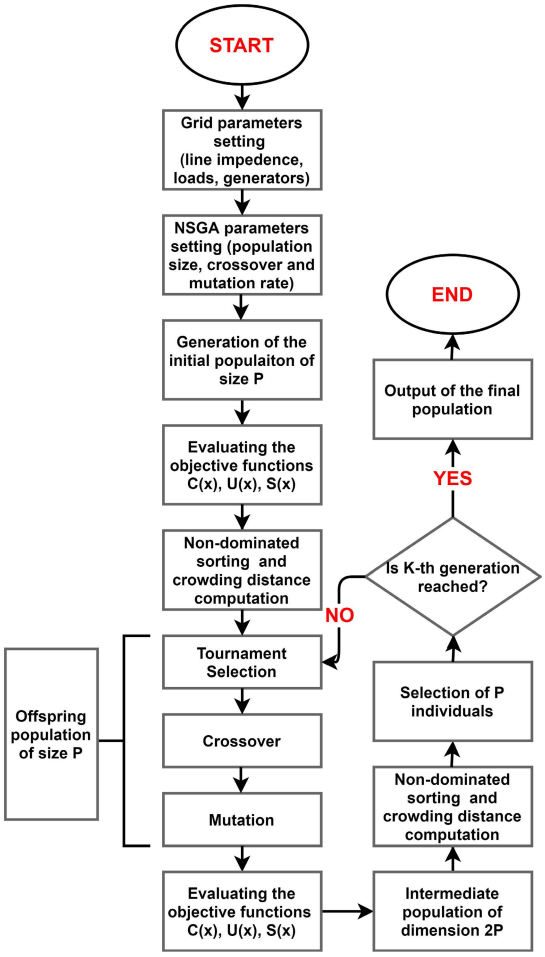

FIGURE 1. Flowchart of the NSGA-II algorithm used to address the multi-objective OPP problem (1).

IV. NSGA-II IMPLEMENTATION AND INITIALIZATION

In multi-objective optimization problems, a solution belongs to the *nondominated set* (also called Pareto or efficient frontier) if there does not exist another solution which performs equal or better with respect to all the chosen objective functions. In practice, only the points belonging to the Pareto set are good candidate solutions for the optimization problem, while the dominated ones are certainly not optimal.

As shortly explained in Sections I and II, due to the multi-objective, nonlinear and combinatorial nature of the OPP problem formalized in Section III, the NSGA-II algorithm provides an effective approach to converge towards the Pareto frontier of $\mathbb{X}$ within a reasonable time. The NSGA-II algorithm selects the members of the next generation by adopting two criteria.

Firstly, the fitness of the parent solutions (the fitter the parent, the more it is likely to survive and to generate offspring) is put into effect by partitioning the population into several subsets called fronts. The first front corresponds to the set of nondominated solutions. The second front corresponds to the set of nondominated solutions if the elements of the

first front are removed from the population, and so forth. This procedure, called *nondominated sorting*, is iterated until all individuals of the population are assigned to one front. Belonging to earlier fronts guarantees a greater chance of survival.

Secondly, when two individuals belong to the same front, the members that are farther from one another (namely with a greater *crowding distance*) are preferred. In this way, the entire front is more likely to be explored.

The flowchart of the proposed NSGA-II implementation, including the aforementioned steps, is shown in Fig. 1.

Similarly to other evolutionary algorithms, the performance and the convergence of NSGA-II depend on the population characteristics as well as the mutation and crossover probabilities. In addition, the selection of a good initial population and the way constraints (1a)-(1c) are implemented is crucial to speed up convergence. As far as the initial population is concerned, a good initial set of feasible solutions is found by solving a sequence of basic single-objective ILP problems based on the same general observability and measurement constraints as the main OPP problem. To this end, first the minimum number of buses $\underline{N}_{PMU}$ to be equipped with PMUs can be found by solving the following ILP subproblem:

$$\underline{N}_{PMU} = \min_{\mathbf{x}\in\mathbb{X}} \ \mathbf{1}^T\mathbf{x} \quad \text{subject to (1a) and (1c).} \tag{12}$$

Then, to create an initial population of given size P, the following ILP satisfiability subproblem is solved iteratively P times, i.e.

$$\begin{aligned} &\min_{\mathbf{x}\in\mathbb{X}} \ \mathbf{0}^T\mathbf{x} \\ &\text{subject to (1a) and (1c)} \\ &\mathbf{1}^T\mathbf{x} = N_{PMU} \\ &\mathbf{D}\mathbf{x} = \mathbf{0} \end{aligned} \tag{13}$$

where N_{PMU} is the initial number of buses to be instrumented with PMUs and it is increased linearly from $\underline{N}_{PMU}$ to N; while $\mathbf{D}$ is a diagonal, binary matrix, including a number of randomly generated unit elements which is kept reasonably smaller than $N - N_{PMU}$ to make the problem feasible. Observe that constraint (1b) is not taken into account in the formalization of subproblems (12) and (13). As a result, the variety of the initial population chosen for NSGA-II optimization is reasonably broad. All individuals are indeed feasible starting points for the main OPP problem provided that no contingencies occur. In (13), the cost function is trivial, since the purpose of this subproblem is just to find a set of well-spread suitable solutions for (1) regardless of their cost. The two further constraints added to subproblem (13) play a complementary role and ensure an adequate diversity of the initial population. In particular, equation $\mathbf{1}^T\mathbf{x} = N_{PMU}$ establishes the number of buses that are instrumented with PMUs. Therefore, by simply changing N_{PMU}, a different member of the initial population results. Equation $\mathbf{D}\mathbf{x} = \mathbf{0}$ prevents instead that a random amount of buses is instrumented with PMUs. In this way, the starting PMU placements obtained by solving (13) multiple times are likely to be different from one another even if the same N_{PMU} value is used. Both ILP subproblems (12) and (13) are simple and converge to feasible solutions quickly by using standard techniques despite their combinatorial nature.

As far as the implementation of constraints (1a)-(1c) is concerned, given that "a major obstacle in the application of genetic algorithms is the embracement of the constraint system" [56], instead of removing or avoiding infeasible solutions, the proposed NSGA-II implementation artificially assigns a large penalty to the solutions violating (1a)-(1c), which makes their survival chances extremely low. To ensure the effectiveness of this procedure, a final check is performed to be sure that the solutions in the Pareto frontier meet constraints (1a)–(1c).

V. OPTIMAL PMU PLACEMENT RESULTS

To test the correct operation and to evaluate the benefits of the proposed tri-objective OPP strategy, multiple simulation results are reported in this Section. They refer to four distribution systems of increasing size, i.e.

- the simple 18-bus distribution system adopted in [57];
- the IEEE 37-bus radial feeder[1];
- the 85-bus network described in [58];
- a 141-bus portion of the distribution grid of the Caracas metropolitan area [59].

Two different instances of the OPP problem (1) (shortly referred to as *Case A* and *Case B* in the following) are solved for each distribution system under test. In particular,

- in *Case A* we have $\mathbf{\Gamma} = \mathbf{I}_N$ and $\mathbf{n_c} = \mathbf{2}$. This is a very conservative, but quite realistic situation in which a PMU is assumed to have no more than two three-phase input channels. Such channels are used to measure the bus voltage phasors and the non-zero injection current phasors, respectively.
- In *Case B* we have that $\mathbf{\Gamma} = \mathbf{A}$ and $\mathbf{n_c} = \mathbf{l} + \mathbf{2}$, where $\mathbf{l}$ is the column vector including the number of lines connected to each bus of the network. In this case, each deployed PMU owns enough channels to measure not only the phasors of bus voltages and injection currents, but also the current phasors of all the lines connected to the bus where a PMU is installed. This assumption holds (often implicitly) in the majority of research works on OPP and it implies that constraint (1c) is always met. In this case, the PMU deployment cost should grow also as a function of the amount of measurement channels.

Case A and *Case B* represent the two extreme cases of a broad range of intermediate possible measurement configurations. In both cases, two further alternative subcases are analyzed depending on whether contingencies are taken into account or not. If no contingencies are considered the OPP problem relies just on constraints (1a) and (1c). Otherwise, constraint (1b) replaces (1a).

[1] http://sites.ieee.org/pes-testfeeders/resources/

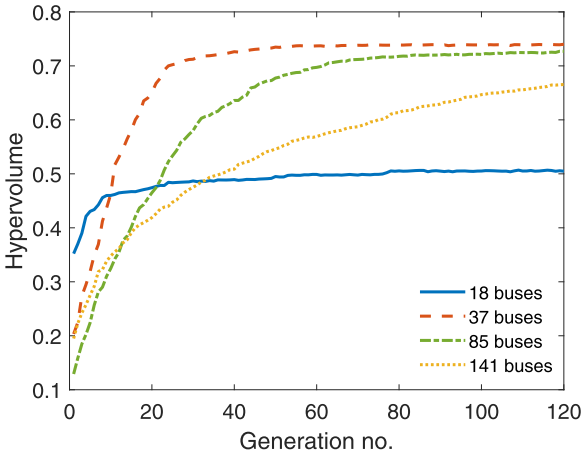

FIGURE 2. Hypervolume curves associated with the optimal PMU placement in the 18-bus, 37-bus, 85-bus and 141-bus distribution systems under study, assuming to use 2-channel PMU only (i.e., in Case A) without including the constraints for contingencies.

In all simulated cases, the parameters of the NSGA-II algorithm were tuned heuristically by following the criteria suggested in [60]. In particular, mutation and crossover probabilities were set equal to 10% and 100%, respectively, since with these values the probability that the optimization algorithm gets stuck in possible local minima is very low. Moreover, the population size P (consisting of 1000 individuals) and the number of generations (i.e., $K = 120$) were chosen after a few iterations to ensure a good convergence to the Pareto frontier in all cases. The convergence of the NSGA-II OPP solver with the aforementioned settings was studied by using the so-called hypervolume method [61].

After scaling all the objective functions to keep their values bounded within [0, 1] (where 0 and 1 correspond to the lowest and the highest values, respectively, returned in all generations), all the obtained feasible solutions are included within a hypercube (i.e., just a cube in the three dimensional case at hand) with hypervolume equal to 1. After each generation, the hypervolume of the portion of space occupied by all obtained solutions (including the dominated ones) is computed. Of course, such a hypervolume is included within the hypercube and generally it tends to grow as the Pareto frontier expands towards the lower edge of the hypercube. When the hypervolume value no longer increases noticeably from a given generation onwards, this means that the Pareto frontier does not change significantly. Therefore, convergence has been reached. Fig. 2 shows the hypervolume curves as a function of the number of generations resulting from OPP in the four distribution systems under study, assuming to use 2-channel PMUs only (i.e., in *Case A*) without including the constraints for contingencies. The results in *Case B* and those with contingency constraints exhibit a similar behavior. Therefore, they have been omitted for the sake of brevity and clarity. Observe that after $K = 120$ generations all hypervolume curves converge to a steady-state value reasonably well although the convergence rate slows down considerably as the grid size grows, as expected.

TABLE 1. OPP computation times (expressed in hours) to reach full convergence with the four distribution systems under study, in both *Case A and Case B with and without including the constraints for contingencies.*

	Computation time [h]			
	Without contingencies		With contingencies	
	Case A	*Case B*	*Case A*	*Case B*
18 buses	7.7	9.3	8.7	10.8
37 buses	13.4	20.4	15.0	22.1
85 buses	43.1	48.3	44.6	57.7
141 buses	58.1	94.9	69.6	112.9

Table 1 reports the OPP computation times for $K = 120$ generations (namely to reach convergence in all the four distribution systems under study) in *Case A* and *Case B* and including either the basic observability constraint or the constraint for contingencies. All simulations were performed on a PC equipped with an Intel Xeon processor E31225 running at 3.10 GHz, 16 GB of memory, a 64-bit operating system and Matlab R2019b.

Quite importantly, the processing times tend to grow almost linearly with the size of the problem. It is worth emphasizing that they are strongly affected by the estimation of the covariance matrices needed to compute functions $\mathsf{U}(\mathbf{x})$ and $\mathsf{S}(\mathbf{x})$, given by (7) and (11), respectively. Indeed, the covariance matrices of the state estimation errors (both expressed in a complex form or in rectangular coordinates) are evaluated through a Monte Carlo approach. The synchrophasors data returned by all PMUs are indeed assumed to be affected by normally distributed random contributions with zero mean and a relative standard deviation such that the TVE is not greater than 1%, in compliance with the steady-state requirements of the IEC/IEEE Standard 60255-118-1:2018 [62]. In practice, this result is obtained if $\sigma_r = 0.0033$. As a consequence, for each member of every generation, the system state is estimated 100 times through (6) by changing randomly the PMU measurement errors. They are assumed to be zero-mean random variables with zero mean and standard deviations expressed into rectangular coordinates as explained in the Appendix. The corresponding state estimation errors result from the differences between the values returned by (6) in every iteration and the actual state values preliminarily computed through the Matpower toolbox [63]. In addition, the maximum sensitivity matrix in (11) is computed by varying the values of the line admittances of each test distribution systems within $\Delta = \pm 20\%$ of their nominal values.

Fig. 3(a)-(d) shows the three-dimensional Pareto frontiers of the solutions obtained with the NSGA-II algorithm in the four test distribution systems under study, assuming that no constraints for contingencies are considered. Each axis is labeled with one of the objective functions (2), (7) and (11). However, the uncertainty values are expressed as a percentage of the nominal slack bus voltage to improve readability. The Pareto frontiers obtained by including the contingency constraints are not shown for the sake of brevity, since they

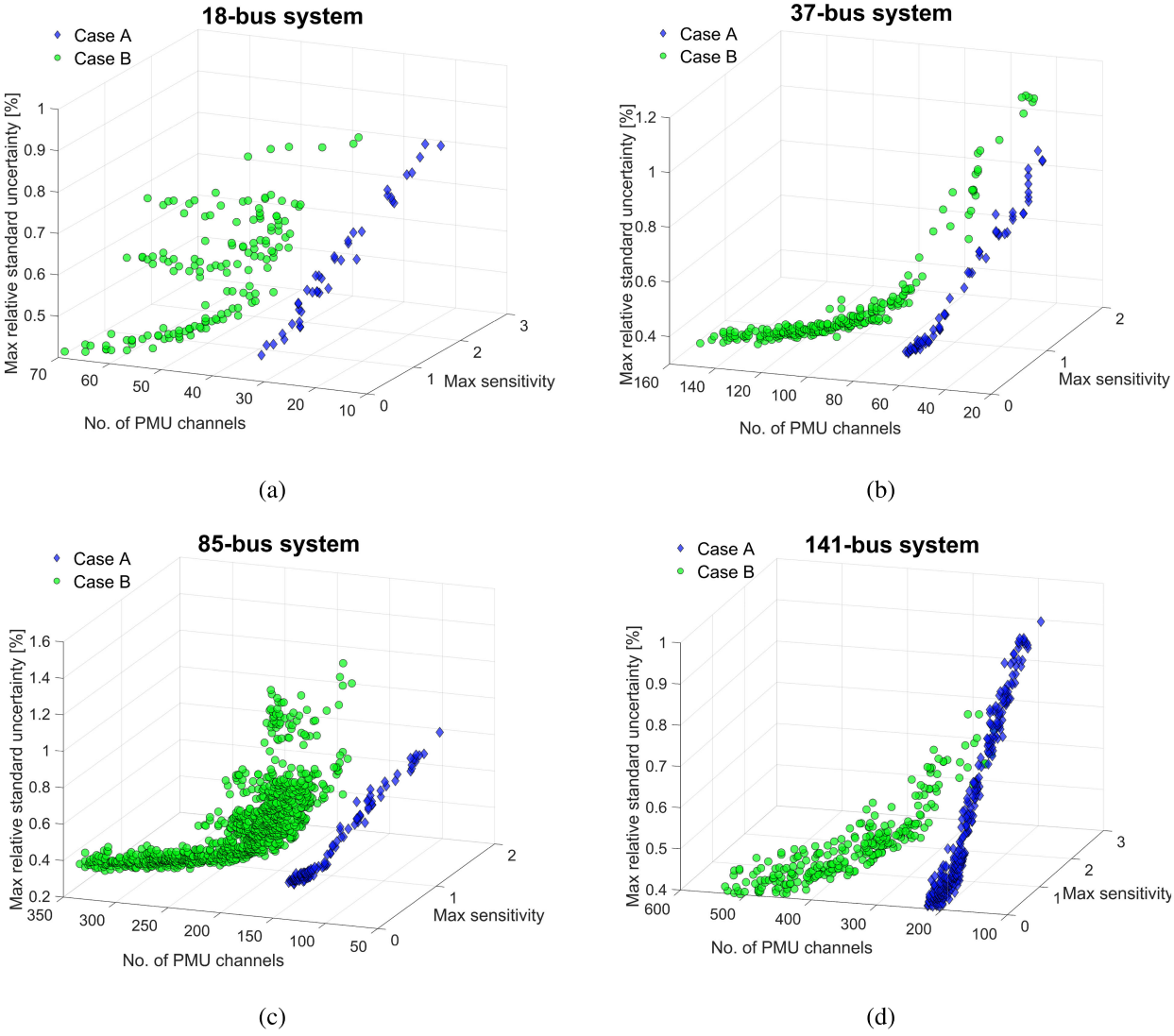

FIGURE 3. Three-dimensional Pareto fronts of the tri-objective OPP based on the proposed NSGA-II algorithm in the 18-bus, 37-bus, 85-bus and 141-bus distribution systems under study. Different markers and colors refer to the measurement configurations labeled as *Case A* and *Case B*, respectively, assuming that no constraints for contingencies are considered.

are almost included in those shown in Fig. 3, as it will be explained shortly. Even though the results in Fig. 3(a)-(d) provide a qualitative rather than a quantitative overview of OPP results, it is worth noticing that

- the Pareto frontiers are quite well-outlined although the inherent granularity of the OPP problem and the chosen population size makes visualization not always clear, especially when the number of PMU locations is close to the minimum value that ensures observability. In such conditions, the values of sensitivity and relative uncertainty tend to grow quickly and quite suddenly, although they are kept bounded;
- in *Case A* the number of PMU channels is evidently bounded by the constraint on the maximum number of channels and on the type of allowed measurements. Nonetheless, state estimation uncertainty and sensitivity do not seem to increase dramatically if compared with *Case B*;
- further results, obtained with different values of σ_r and omitted for the sake of brevity, confirm that the maximum state uncertainty values of the Pareto frontier scale accordingly, as expected;
- the projections of the Pareto frontiers onto plane $(\mathsf{S}(\mathbf{x}), \mathsf{U}(\mathbf{x}))$ confirm that by increasing the number of PMU channels, both maximum sensitivity and maximum state estimation uncertainty tend to decrease, thus converging to the solutions clustered around the bottom left corner of all plots.

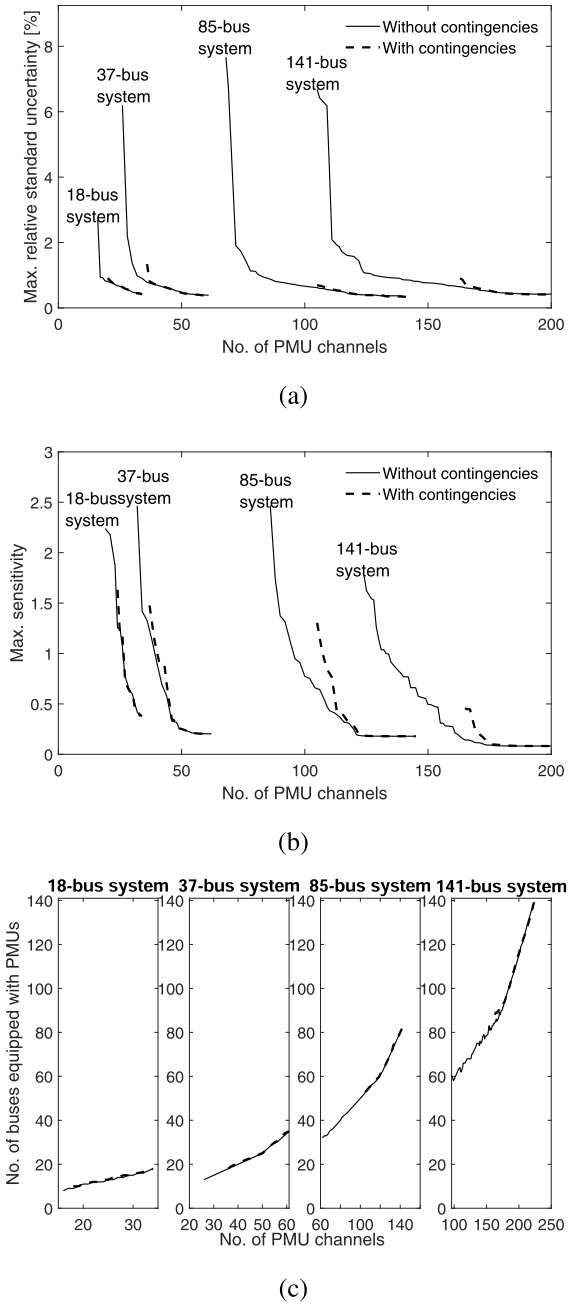

FIGURE 4. Lower envelopes of the projections onto planes (C(**x**), U(**x**)) in (a) and (C(**x**), S(**x**)) in (b) of the Pareto frontiers of the *Case A* OPP solutions in the four distribution systems under study. In (c) the number of buses instrumented with PMUs in either system is plotted as a function of the total number of PMU channels used for grid monitoring. Dashed and solid lines refer to the results obtained with and without the constraints for contingencies, respectively.

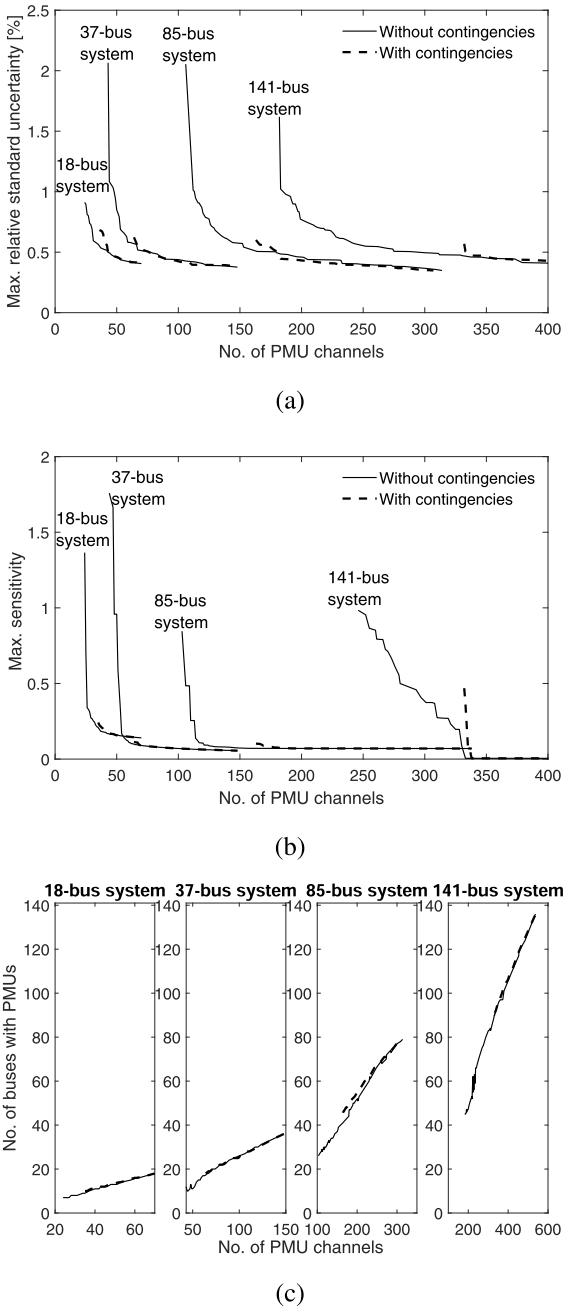

FIGURE 5. Lower envelopes of the projections onto planes (C(**x**), U(**x**)) in (a) and (C(**x**), S(**x**)) in (b) of the Pareto frontiers of the *Case B* OPP solutions in the four distribution systems under study. In (c) the number of buses instrumented with PMUs in either system is plotted as a function of the total number of PMU channels used for grid monitoring. Dashed and solid lines refer to the results obtained with and without the constraints for contingencies, respectively.

A more quantitative insight into the trade-offs between the OPP solutions obtained with the proposed tri-objective approach can be deduced from the curves shown in Figs. 4 and 5, which refer to *Case A* and *Case B*, respectively. In Figs. 4(a)-(b) and 5(a)-(b), the lower envelopes of the projections of the three-dimensional Pareto frontiers onto orthogonal planes $(\mathsf{C}(\mathbf{x}), \mathsf{U}(\mathbf{x}))$ and $(\mathsf{C}(\mathbf{x}), \mathsf{S}(\mathbf{x}))$, respectively, are plotted. The number of buses actually instrumented with PMUs in the considered distribution systems is instead shown in Figs. 4(c) and 5(c) as a function of the number of PMU channels. Observe that the curves obtained with (dashed lines) and without (solid lines) the constraints for contingencies are shown. The curves in Figs. 4 and 5 provide some interesting and quite general information on PMU placement. The main remarks are summarized below.

- If no constraints for possible contingencies are considered, once the number of PMUs is large enough to guarantee basic system observability, both the maximum standard estimation uncertainty and the maximum sensitivity tend to decrease quite sharply in both *Case A* and *Case B* as the number of PMU channels grows. This trend is consistent with some previous research results, although they were obtained in totally different and largely suboptimal conditions and with a different (i.e., nonlinear) state estimator [64], [65]. The curves obtained using smaller distribution systems look steeper. This behavior is due to the fact that the impact of any new PMU measurement on state estimation is stronger in small systems than in large ones. Figs. 4(a)-(b) and 5(a)-(b) show that the law of diminishing returns holds: when the total number of PMU channels is between about 150% and 200% of the number of grid buses, the decrease of both the maximum state estimation relative uncertainty and the maximum sensitivity to line tolerances becomes negligible. Therefore, increasing the number of deployed PMUs beyond given thresholds (depending on the constraints of the channels that can be used) is quite pointless, as it would just lead to higher costs with no benefits.
- The values of $\mathsf{U}(\mathbf{x})$ and $\mathsf{S}(\mathbf{x})$ in *Case A* are larger than those in *Case B*, as expected, due to the additional current phasor measurements used for state estimation in the latter case. However, if the number of measurements (namely the PMU channels) is large enough, the maximum uncertainty and sensitivity curves tend to converge to the same respective values.
- It is important to highlight that the number of PMU channels should not be confused with the number of PMU locations and, consequently, with the number of measuring devices to be installed [provided that they all have the maximum number of channels imposed by constraint (1c)]. The curves in Figs. 4(a)-(b) and 5(a)-(b) shows that the number of PMU channels in *Case B* is always larger than in *Case A*, as expected. However, the minimum number of grid buses monitored by a PMU in *Case B* is generally slightly smaller than in *Case A*. This is visible by comparing Figs. 4(c) and 5(c), and it is reasonable because the full availability of measurement channels in *Case B* supports system observability. In particular, if no constraints for contingencies are included in the problem, system observability of all systems under study can be obtained by instrumenting $39\% \pm 5\%$ or $32\% \pm 5\%$ of grid buses in *Case A* and in *Case B*, respectively. These values depend not only on network structure, but also on the number and the positions of ZI buses in the system.
- Quite interestingly, once the minimum number of PMU locations and PMU channels satisfying constraint (1b) is found, both the maximum state estimation relative uncertainty and the maximum sensitivity curves are almost overlapped with those computed without the constraints for contingencies. This result is consistent with the fact that constraint (1b) is stricter than (1a). Therefore, the solutions in the Pareto frontiers obtained including the constraints for contingencies are likely to be subsets of the solutions obtained with the basic observability constraint. Moreover, a solution of the Pareto frontier that meets constraint (1b) generally ensures also that the values of $\mathsf{U}(\mathbf{x})$ and $\mathsf{S}(\mathbf{x})$ are steadily close to the respective lowest asymptotic values. In addition, the minimum number of buses that need to be instrumented with PMUs as well as the corresponding number of channels becomes larger. This is quite obvious because providing observability in the case of single-line faults or losses of PMU data requires measurement redundancy. In such conditions, between at least about 50% and 60% of all buses have to be monitored by PMUs.

It is worth mentioning that no clear connection was found between PMU placement results and maximum state estimation uncertainty or sensitivity to line parameter tolerances. We have just observed that for a given instance of the OPP problem, between 15% and 20% of buses are included in almost all the Pareto frontier solutions. The set of common PMU locations comprises always the slack bus or an adjacent node, while all the others are quite evenly spread over every considered grid.

VI. AN EXAMPLE OF COST ANALYSIS

To complete the present research, four meaningful OPP results in both *Case A* and *Case B* are reported in Table 2(a)-(d) for the 18-bus, 37-bus, 85-bus and 141-bus distribution systems, respectively. Such OPP results correspond to the points of the Pareto frontier envelopes shown in Figs. 4(a)-(b) and 5(a)-(b) for which both the maximum state estimation standard uncertainty and its maximum sensitivity to line parameter tolerances reach approximately the respective lowest asymptotic values both with and without including the constraints for contingencies. More in details,

- in *Case A* the solutions of the Pareto frontiers that rely on 24, 50, 120 and 155 PMU channels for the 18-bus, 37-bus, 85-bus and 141-bus system, respectively, are chosen.
- Similarly, in *Case B* we consider the solutions of the Pareto frontiers for which 47 PMU channels (18-bus system), 71 PMU channels (37-bus system), 180 PMU channels (85-bus system) or 332 PMU channels (141-bus system) are used.

Table 2(a)-(d) summarizes not only the bus numbers where the PMUs are actually installed, but also their number of channels. Note that both low state estimation uncertainty and low sensitivity to line parameters tolerances are achieved even if the PMUs are not installed at every bus. In fact, in *Case A* between about 30% and 40% of buses (i.e., 6, 12, 24 and 60 out of 18, 37, 85 and 141 buses, respectively) are not equipped with a PMU. This result is probably due to the presence of

TABLE 2. Examples of OPP results for the 18-bus (a), 37-bus (b), 85-bus (c) and 141-bus (d) distribution systems under study in both *Case A* and *Case B*. With either set of constraints on the measurement channels, the reported PMU placement refers to the point of the Pareto frontiers for which the maximum standard estimation uncertainty and the maximum sensitivity to line parameter tolerances are close to the respective minimal values, while the total number of PMU channels is kept as small as possible.

	Bus type	Quantity	Bus numbers
Case A	Buses without PMUs	6	2, 3, 4, 9, 13, 15
	Buses with 2 PMU channels	12	1, 5, 6, 7, 8, 10, 11, 12, 14, 16, 17, 18
Case B	Buses without PMUs	6	2, 3, 5, 7, 11, 18
	Buses with 3 PMU channels	4	1, 10, 14, 16
	Buses with 4 PMU channels	5	6, 8, 9, 12, 17
	Buses with 5 PMU channels	3	4, 13, 15

(a)

	Bus Type	Quantity	Bus numbers
Case A	Buses without PMUs	12	22, 27, 28, 29, 30, 31, 32, 33, 34, 35, 36, 37
	Buses with 2 PMU channels	25	1, 2, 3, 4, 5, 6, 7, 8, 9, 10, 11, 12, 13, 14, 15, 16, 17, 18, 19, 20, 21, 23, 24, 25, 26
Case B	Buses without PMUs	17	15, 17, 18, 20, 22, 26, 27, 28, 29, 30, 31, 32, 33, 34, 35, 36, 37
	Buses with 3 PMU channels	10	1, 3, 6, 8, 9, 12, 16, 19, 23, 25
	Buses with 4 PMU channels	9	2, 4, 5, 10, 11, 13, 14, 21, 24
	Buses with 5 PMU channels	1	7

(b)

	Bus type	Quantity	Bus numbers
Case A	Buses without PMUs	24	2, 3, 5, 7, 8, 9, 10, 12, 13, 27, 29, 32, 34, 35, 41, 48, 49, 52, 58, 64, 65, 67, 70, 81
	Buses with 1 PMU channel	2	68, 73
	Buses with 2 PMU channels	59	All the others
Case B	Buses without PMUs	38	All the others
	Buses with 3 PMU channels	21	1, 15, 16, 17, 36, 38, 47, 51, 54, 55, 56, 59, 62, 66, 72, 74, 75, 78, 82, 84, 85
	Buses with 4 PMU channels	14	4, 6, 11, 21, 31, 44, 46, 50, 53, 57, 61, 63, 80, 82
	Buses with 5 PMU channels	11	2, 3, 5, 8, 19, 26, 29, 32, 41, 48, 70
	Buses with 6 PMU channels	1	67

(c)

	Bus type	Quantity	Bus numbers
Case A	Buses without PMUs	60	2, 3, 4, 5, 6, 7, 10, 11, 14, 15, 16, 17, 19, 22, 24, 25, 26, 28, 31, 33, 38, 40, 42, 43, 45, 46, 47 50, 54, 55, 57, 60, 61, 63, 64, 70, 78, 79, 81, 85, 87, 88, 90, 91, 92, 93, 95, 97, 99, 101, 103 108, 118, 119, 120, 121, 122, 124, 125, 126
	Buses with 1 PMU channel	7	18, 30, 102, 104, 114, 115, 131
	Buses with 2 PMU channels	74	All the others
Case B	Buses without PMUs	50	All the others
	Buses with 3 PMU channels	44	1, 32, 34, 35, 36, 52, 53, 59, 62, 68, 69, 71, 72, 74, 75, 77, 80, 82, 83, 84, 87, 98, 100, 105, 106 107, 109, 110, 111, 112, 113, 116, 117, 130, 132, 133, 134, 135, 136, 137, 138, 139, 140, 141
	Buses with 4 PMU channels	36	8, 9, 12, 20, 21, 27, 29, 37, 39, 40, 41, 48, 51, 54, 56, 57, 58, 61, 64, 65, 66, 67, 73, 76, 86, 88 96, 101, 103, 108, 115, 123, 124, 127, 128, 129
	Buses with 5 PMU channels	10	13, 18, 23, 44, 49, 63, 79, 89, 104, 119
	Buses with 6 PMU channels	1	94

(d)

ZI buses. In *Case B* the share of buses without PMUs is slightly higher on average, i.e., from 32% to 46% depending on network topology.

It is worth recalling that *Case A* and *Case B* represent the extremes of a broad range of possible measurement configurations depending on how constraint (1c) is actually implemented. Of course, by changing constraint (1c) the actual deployment costs may change considerably as a function not only of the amount of installed PMUs, but also on the number of their channels. Unfortunately, an accurate comparative cost analysis of alternative PMU placement strategies can be hardly done due to both the large variety of context-specific factors and the huge differences between transmission and distribution systems. Indeed, according to a study of the U.S. Department of Energy, the overall PMU deployment cost per measurement point at the transmission level (including procurement, installation and commissioning) ranges from about 40000 $ up to 180000 $ [47], with just a limited fraction of the total amount due to measurement devices. This range is quite large although it ''does not reflect differences among utilities in required phasor data concentrators, communications infrastructure upgrades, applications costs, staff training needs, and physical substation constraints to installing PMUs'' [47].

At the distribution level, the overall PMU deployment cost per measurement point is even unclearer, as just pilot installations have been proposed so far. However, it should be at least about one order of magnitude lower than the cost at the transmission level to ensure a widespread use of PMUs. Due to the lack of trustworthy general information on procurement, installation, and commissioning costs at the distribution level, only the bare instrumental costs will be considered in the present analysis. In particular, two alternative scenarios are analyzed, i.e.

- A traditional scenario based on classic multi-channel PMUs (like those used in transmission systems);
- A possible future scenario in which specific distribution-oriented micro-PMUs are used.

In the former scenario, a base PMU cost of 20000 $ plus 3000 $ per channel is considered [17]. In the latter one, the cost of a micro-PMU can be assumed equal to 3500 $, as reported in [7]. According to device specifications, micro-PMUs include 8 input lines. However, considering that the phasors to be measured usually refer to three-phase voltage and/or currents (possibly including a neutral connection), no more than 2 three-phase measurements can be performed with a single device. Therefore, in *Case B* about $\lceil \frac{n_{c_i}}{2} \rceil$ micro-PMUs (where $\lceil \cdot \rceil$ is the function returning the smallest integer value that is greater than or equal to its argument) have to be installed at bus i if n_{c_i} channels are needed.

The results of the cost analysis in the two aforementioned scenarios in both *Case A* and *Case B* for the OPP solutions shown in Table 2(a)-(d) are summarized in Table 3. All amounts are expressed in thousands of USD and no scale economies are assumed. As expected, the costs associated with micro-PMU placement are much lower than those resulting from traditional PMU installation. Quite interestingly, the use of more than two PMU measurements per bus (i.e., *Case B*) usually is not profitable. As soon as the values of maximum state estimation uncertainty and the maximum sensitivity to line parameter tolerances are low enough (possibly with some redundancy to take contingencies into account) adding further current phasor measurements usually just increases the total costs with no benefits. Therefore, the measurement constraint (1c) specified in *Case A* is generally preferable. The only exceptions occur when traditional multi-channel PMUs are deployed in the 37-bus and 85-bus systems because in such cases the increase in the number of buses without PMUs from about 30% in *Case A* to about 45% in *Case B* is greater than in the other systems under test and it is large enough to counterbalance the additional costs due to the larger total amount of PMU channels. Nevertheless, such an increase in the number of buses that are not instrumented is not enough to make *Case B* profitable when the 2-channel micro-PMUs are used, since the total number of micro-PMUs that have to be installed is globally greater than in *Case A*.

TABLE 3. Examples of total instrumental costs (expressed in thousands of USD) associated with the optimal PMU placements shown in Table 2(a)-(d) in both *Case A* and *Case B*, assuming to use either classic transmission-oriented multi-channel PMUs or cheaper distribution oriented 2-channel micro-PMUs.

	Multi-channel PMUs		2-channel micro-PMUs	
	Case A	*Case B*	*Case A*	*Case B*
18-bus system	312	381	42	94.5
37-bus system	650	613	87.5	143.5
85-bus system	1580	1480	213.5	371
141-bus system	2085	2816	283.5	675.5

VII. CONCLUSION

In this paper, the issue of installing Phasor Measurement Units (PMUs) is addressed from a novel perspective, i.e. by solving a tri-objective optimization problem whose objective functions are: the total number of PMU channels, the maximum state estimation uncertainty based only on high-rate PMU measurements, and the maximum state estimation sensitivity to line parameter tolerances. In addition, constraints on system observability (both with and without considering constraints for contingencies) as well as on the number of PMU channels and on the type of allowed PMU measurements at every bus are included in the problem formulation. The tri-objective optimization problem is solved through a custom implementation of the genetic algorithm NSGA-II. Other heuristic optimization algorithms could maybe perform even better from the computational point of view. Nevertheless, no significant changes are expected either in the results or in the conclusions, since the proposed NSGA-II algorithm clearly converges to the Pareto frontiers of interest in all distribution systems under test. Indeed, the focus of our study is on distribution systems, due to the

growing interest in a widespread PMU deployment to support smart grid operation. The results obtained using four test distribution systems consisting of 18, 37, 85 and 141 buses, respectively, reveal that if the number of buses instrumented with PMUs exceeds given thresholds, the reduction of maximum state estimation uncertainty and maximum sensitivity to line parameter tolerances becomes negligible, while the instrumental costs tend to grow considerably. The results obtained with the four distribution systems under study suggest that between about 30% and 40% of all buses can be left unmonitored even if PMUs with just two measurement channels are used. This fraction may grow by some percent if no constraints exist on the number of PMU channels. However, the latter choice usually is not economically profitable and does not provide significant improvements in state estimation. Quite interestingly, an optimal PMU placement configuration able to ensure small state estimation uncertainty and sensitivity is likely to be robust to contingencies as well.

A topic for future research could be the application of multi-criteria decision analysis methodologies such as, for instance, the multi-attribute value theory (MAVT), to find a unique "best" placement from the three dimensional set of nondominated solutions. The use of these techniques may also provide a way to integrate the decision makers' expertise and preferences into an otherwise merely automatic procedure.

APPENDIX - VARIANCE OF PMU MEASUREMENT DATA IN RECTANGULAR COORDINATES

Let z_X denote a generic current or voltage phasor measured by a PMU where subscript X is replaced by V or I in (3) depending on whether a voltage or a current phasor is measured. Since PMU data are typically expressed in polar coordinates, any measured quantity can be rewritten as $z_X = (X + \varepsilon_X)e^{j(\varphi_X + \varepsilon_{\varphi_X})}$, where X and φ_X are the actual values of phasor magnitude and phase, while ε_X and ε_{φ_X} are the corresponding measurement uncertainty contributions. If a polar-to-rectangular coordinates transformation is performed, then the pair of real and imaginary parts of the phasor data used for state estimation given by (3)-(6) can be rewritten as

$$\begin{aligned} z_{X_R} &= (X + \varepsilon_X)\cos(\varphi_X + \varepsilon_{\varphi_X}) = \qquad \text{(A.1)} \\ &= (X + \varepsilon_X)[\cos\varphi_X \cos\varepsilon_{\varphi_X} - \sin\varphi_X \sin\varepsilon_{\varphi_X}] \\ z_{X_I} &= (X + \varepsilon_X)\sin(\varphi_X + \varepsilon_{\varphi_X}) = \qquad \text{(A.2)} \\ &= (X + \varepsilon_X)[\sin\varphi_X \cos\varepsilon_{\varphi_X} + \cos\varphi_X \sin\varepsilon_{\varphi_X}]. \end{aligned}$$

Let us assume that, due to the superimposition of multiple uncertainty contributions, both ε_X and ε_{φ_X} can be modeled as two zero-mean normally distributed random variables with variances σ_X^2 and $\sigma_{\varphi_X}^2$, respectively. Since the maximum TVE of a PMU must be lower than 1% (usually quite evenly split between magnitude and phase errors) [62], both ε_X and ε_{φ_X} are small enough to assume that in (A.1) and (A.2) i) $\sin\varepsilon_{\varphi_X} \approx \varepsilon_{\varphi_X}$ and ii) all terms proportional to $\varepsilon_X \sin\varepsilon_{\varphi_X} \approx \varepsilon_X\varepsilon_{\varphi_X}$ are negligible. Hence, if these approximations are used to compute the variance of z_{X_R} and z_{X_I}, after simple algebraic manipulations it results that

$$\begin{aligned} \sigma_{X_R}^2 &= \mathbb{E}(z_{X_R} - \mathbb{E}(z_{X_R})^2) = \qquad \text{(A.3)} \\ &= X^2\sigma_{\varphi_X}^2 \sin^2\varphi_X + \sigma_X^2 \cos^2\varphi_X - X\rho\sigma_X\sigma_{\varphi_X} \sin 2\varphi_X \end{aligned}$$

and

$$\begin{aligned} \sigma_{X_I}^2 &= \mathbb{E}(z_{X_I} - \mathbb{E}(z_{X_I})^2) = \qquad \text{(A.4)} \\ &= X^2\sigma_{\varphi_X}^2 \cos^2\varphi_X + \sigma_X^2 \sin^2\varphi_X + X\rho\sigma_X\sigma_{\varphi_X} \sin 2\varphi_X \end{aligned}$$

where $|\rho| \leq 1$ is the correlation coefficient between ε_X and ε_{φ_X} due to the fact that the same device is used to measure both phasor magnitude and angle. Expressions (A.3)-(A.4) can be finally used to compute the elements of matrix $\mathbf{R}$ in (6), (9) and (10), once the uncertainties of PMU phasor magnitude and angle in polar coordinates are known.

REFERENCES

[1] J. De La Ree, V. Centeno, J. S. Thorp, and A. G. Phadke, "Synchronized phasor measurement applications in power systems," *IEEE Trans. Smart Grid*, vol. 1, no. 1, pp. 20–27, Jun. 2010.

[2] D. Macii, G. Barchi, and D. Petri, "Design criteria of digital filters for synchrophasor estimation," in *Proc. IEEE Int. Instrum. Meas. Technol. Conf. (I2MTC)*, May 2013, pp. 1579–1584.

[3] S. M. Blair, M. H. Syed, A. J. Roscoe, G. M. Burt, and J.-P. Braun, "Measurement and analysis of PMU reporting latency for smart grid protection and control applications," *IEEE Access*, vol. 7, pp. 48689–48698, 2019.

[4] K. Deb, A. Pratap, S. Agarwal, and T. Meyarivan, "A fast and elitist multiobjective genetic algorithm: NSGA-II," *IEEE Trans. Evol. Comput.*, vol. 6, no. 2, pp. 182–197, Apr. 2002.

[5] S. Bandyopadhyay and R. Bhattacharya, "Solving a tri-objective supply chain problem with modified NSGA-II algorithm," *J. Manuf. Syst.*, vol. 33, no. 1, pp. 41–50, Jan. 2014.

[6] J. Sexauer, P. Javanbakht, and S. Mohagheghi, "Phasor measurement units for the distribution grid: Necessity and benefits," in *Proc. IEEE PES Innov. Smart Grid Technol. Conf. (ISGT)*, Washington, DC, USA, Feb. 2013, pp. 1–6.

[7] A. von Meier, E. Stewart, A. McEachern, M. Andersen, and L. Mehrmanesh, "Precision micro-synchrophasors for distribution systems: A summary of applications," *IEEE Trans. Smart Grid*, vol. 8, no. 6, pp. 2926–2936, Nov. 2017.

[8] P. Romano, M. Paolone, T. Chau, B. Jeppesen, and E. Ahmed, "A high-performance, low-cost PMU prototype for distribution networks based on FPGA," in *Proc. IEEE Manchester PowerTech*, Manchester, U.K., Jun. 2017, pp. 1–6.

[9] R. F. Nuqui and A. G. Phadke, "Phasor measurement unit placement techniques for complete and incomplete observability," *IEEE Trans. Power Del.*, vol. 20, no. 4, pp. 2381–2388, Oct. 2005.

[10] T. L. Baldwin, L. Mili, M. B. Boisen, and R. Adapa, "Power system observability with minimal phasor measurement placement," *IEEE Trans. Power Syst.*, vol. 8, no. 2, pp. 707–715, May 1993.

[11] B. Xu and A. Abur, "Observability analysis and measurement placement for systems with PMUs," in *Proc. IEEE PES Power Syst. Conf. Expo.*, Oct. 2004, pp. 943–946.

[12] J. Chen and A. Abur, "Improved bad data processing via strategic placement of PMUs," in *Proc. IEEE Power Eng. Soc. Gen. Meeting*, Jun. 2005, pp. 509–513.

[13] J. Chen and A. Abur, "Placement of PMUs to enable bad data detection in state estimation," *IEEE Trans. Power Syst.*, vol. 21, no. 4, pp. 1608–1615, Nov. 2006.

[14] R. Kavasseri and S. K. Srinivasan, "Joint optimal placement of PMU and conventional measurements in power systems," in *Proc. IEEE Int. Symp. Circuits Syst.*, Paris, France, May 2010, pp. 3449–3452.

[15] B. Gou, "Generalized integer linear programming formulation for optimal PMU placement," *IEEE Trans. Power Syst.*, vol. 23, no. 3, pp. 1099–1104, Aug. 2008.

[16] S. Azizi, G. B. Gharehpetian, and A. S. Dobakhshari, "Optimal integration of phasor measurement units in power systems considering conventional measurements," *IEEE Trans. Smart Grid*, vol. 4, no. 2, pp. 1113–1121, Jun. 2013.

[17] M. Ghamsari-Yazdel and M. Esmaili, "Reliability-based probabilistic optimal joint placement of PMUs and flow measurements," *Int. J. Electr. Power Energy Syst.*, vol. 78, pp. 857–863, Jun. 2016.
[18] J. Liu, J. Tang, F. Ponci, A. Monti, C. Muscas, and P. A. Pegoraro, "Trade-offs in PMU deployment for state estimation in active distribution grids," *IEEE Trans. Smart Grid*, vol. 3, no. 2, pp. 915–924, Jun. 2012.
[19] Z. Wu, X. Du, W. Gu, Y. Liu, P. Ling, J. Liu, and C. Fang, "Optimal PMU placement considering load loss and relaying in distribution networks," *IEEE Access*, vol. 6, pp. 33645–33653, 2018.
[20] S.-E. Razavi, H. Falaghi, C. Singh, J. Aghaei, and A. E. Nezhad, "A novel linear framework for phasor measurement unit placement considering the effect of adjacent zero-injection buses," *Measurement*, vol. 133, pp. 532–540, Feb. 2019.
[21] C. Lu, Z. Wang, M. Ma, R. Shen, and Y. Yu, "An optimal PMU placement with reliable zero injection observation," *IEEE Access*, vol. 6, pp. 54417–54426, 2018.
[22] C. Rakpenthai, S. Premrudeepreechacharn, S. Uatrongjit, and N. R. Watson, "An optimal PMU placement method against measurement loss and branch outage," *IEEE Trans. Power Del.*, vol. 22, no. 1, pp. 101–107, Jan. 2007.
[23] F. Aminifar, A. Khodaei, M. Fotuhi-Firuzabad, and M. Shahidehpour, "Contingency-constrained PMU placement in power networks," *IEEE Trans. Power Syst.*, vol. 25, no. 1, pp. 516–523, Feb. 2010.
[24] R. Sodhi, S. C. Srivastava, and S. N. Singh, "Optimal PMU placement to ensure system observability under contingencies," in *Proc. IEEE Power Energy Soc. Gen. Meeting*, Jul. 2009, pp. 1–6.
[25] R. Emami and A. Abur, "Robust measurement design by placing synchronized phasor measurements on network branches," *IEEE Trans. Power Syst.*, vol. 25, no. 1, pp. 38–43, Feb. 2010.
[26] X.-C. Guo, C.-S. Liao, and C.-C. Chu, "Enhanced optimal PMU placements with limited observability propagations," *IEEE Access*, vol. 8, pp. 22515–22524, 2020.
[27] S. Kumar, B. Tyagi, V. Kumar, and S. Chohan, "Optimization of phasor measurement units placement under contingency using reliability of network components," *IEEE Trans. Instrum. Meas.*, vol. 69, no. 12, pp. 9893–9906, Dec. 2020.
[28] J. Huang, N. E. Wu, and M. C. Ruschmann, "Data-availability-constrained placement of PMUs and communication links in a power system," *IEEE Syst. J.*, vol. 8, no. 2, pp. 483–492, Jun. 2014.
[29] M. Shafiullah, M. I. Hossain, M. A. Abido, T. Abdel-Fattah, and A. H. Mantawy, "A modified optimal PMU placement problem formulation considering channel limits under various contingencies," *Measurement*, vol. 135, pp. 875–885, Mar. 2019.
[30] Z. Miljanić, I. Djurović, and I. Vujošević, "Optimal placement of PMUs with limited number of channels," *Electr. Power Syst. Res.*, vol. 90, pp. 93–98, Sep. 2012.
[31] M. Korkali and A. Abur, "Impact of network sparsity on strategic placement of phasor measurement units with fixed channel capacity," in *Proc. IEEE Int. Symp. Circuits Syst.*, May 2010, pp. 3445–3448.
[32] M. H. Rezaeian Koochi, P. Dehghanian, and S. Esmaeili, "PMU placement with channel limitation for faulty line detection in transmission systems," *IEEE Trans. Power Del.*, vol. 35, no. 2, pp. 819–827, Apr. 2020.
[33] N. M. Manousakis and G. N. Korres, "Optimal allocation of phasor measurement units considering various contingencies and measurement redundancy," *IEEE Trans. Instrum. Meas.*, vol. 69, no. 6, pp. 3403–3411, Jun. 2020.
[34] S. Chakrabarti, D. Eliades, E. Kyriakides, and M. Albu, "Measurement uncertainty considerations in optimal sensor deployment for state estimation," in *Proc. IEEE Int. Symp. Intell. Signal Process.*, Oct. 2007, pp. 1–6.
[35] Z. Hong-Shan, L. Ying, M. Zeng-qiang, and Y. Lei, "Sensitivity constrained PMU placement for complete observability of power systems," in *Proc. IEEE/PES Transmiss. Distrib. Conf. Expo.: Asia–Pacific*, Aug. 2005, pp. 1–5.
[36] S. M. Mazhari, H. Monsef, H. Lesani, and A. Fereidunian, "A multi-objective PMU placement method considering measurement redundancy and observability value under contingencies," *IEEE Trans. Power Syst.*, vol. 28, no. 3, pp. 2136–2146, Aug. 2013.
[37] C. Peng, H. Sun, and J. Guo, "Multi-objective optimal PMU placement using a non-dominated sorting differential evolution algorithm," *Int. J. Electr. Power Energy Syst.*, vol. 32, no. 8, pp. 886–892, Oct. 2010.
[38] N. M. Manousakis, G. N. Korres, and P. S. Georgilakis, "Taxonomy of PMU placement methodologies," *IEEE Trans. Power Syst.*, vol. 27, no. 2, pp. 1070–1077, May 2012.
[39] B. Milosevic and M. Begovic, "Nondominated sorting genetic algorithm for optimal phasor measurement placement," *IEEE Trans. Power Syst.*, vol. 18, no. 1, pp. 69–75, Feb. 2003.
[40] Y.-F. Huang, S. Werner, J. Huang, N. Kashyap, and V. Gupta, "State estimation in electric power grids: Meeting new challenges presented by the requirements of the future grid," *IEEE Signal Process. Mag.*, vol. 29, no. 5, pp. 33–43, Sep. 2012.
[41] P. A. Pegoraro and S. Sulis, "Robustness-oriented meter placement for distribution system state estimation in presence of network parameter uncertainty," *IEEE Trans. Instrum. Meas.*, vol. 62, no. 5, pp. 954–962, May 2013.
[42] M. K. Arpanahi, H. H. Alhelou, and P. Siano, "A novel multiobjective OPP for power system small signal stability assessment considering WAMS uncertainties," *IEEE Trans. Ind. Informat.*, vol. 16, no. 5, pp. 3039–3050, May 2020.
[43] M. Nazari-Heris and B. Mohammadi-Ivatloo, "Application of heuristic algorithms to optimal PMU placement in electric power systems: An updated review," *Renew. Sustain. Energy Rev.*, vol. 50, pp. 214–228, Oct. 2015.
[44] M. Nazari-Heris and B. Mohammadi-Ivatloo, "Optimal placement of phasor measurement units to attain power system observability utilizing an upgraded binary harmony search algorithm," *Energy Syst.*, vol. 6, no. 2, pp. 201–220, Jun. 2015.
[45] K. Deb, L. Thiele, M. Laumanns, and E. Zitzler, "Scalable test problems for evolutionary multiobjective optimization," in *Evolutionary Multiobjective Optimization*. London, U.K.: Springer, 2005, pp. 105–145.
[46] M. Ghamsari-Yazdel, M. Esmaili, and N. Amjady, "Optimal substation-based joint allocation of PMUs and measuring channels considering network expansion planning," *Int. J. Electr. Power Energy Syst.*, vol. 106, pp. 274–287, Mar. 2019.
[47] U. S. relax Department of Energy. (Oct. 2014). *Factors Affecting PMU Installation Costs–Smart Grid Investment Gran Program*. https://www.energy.gov/oe/downloads/factors-affecting-pmu-installation-costs-october-2014
[48] BIPM, IEC, IFCC, ILAC, ISO, IUPAC, IUPAP, and OIML, *Evaluation of Measurement Data—Guide to the Expression of Uncertainty in Measurement*, document JCGM 100:2008, JCGM, Sep. 2008.
[49] S. Soni, S. Bhil, D. Mehta, and S. Wagh, "Linear state estimation model using phasor measurement unit (PMU) technology," in *Proc. 9th Int. Conf. Electr. Eng., Comput. Sci. Autom. Control (CCE)*, Mexico City, Mexico, Sep. 2012, pp. 1–6.
[50] S. Sarri, L. Zanni, M. Popovic, J.-Y. Le Boudec, and M. Paolone, "Performance assessment of linear state estimators using synchrophasor measurements," *IEEE Trans. Instrum. Meas.*, vol. 65, no. 3, pp. 535–548, Mar. 2016.
[51] J. Song, E. Dall'Anese, A. Simonetto, and H. Zhu, "Dynamic distribution state estimation using synchrophasor data," *IEEE Trans. Smart Grid*, vol. 11, no. 1, pp. 821–831, Jan. 2020.
[52] D. Della Giustina, M. Pau, P. A. Pegoraro, F. Ponci, and S. Sulis, "Electrical distribution system state estimation: Measurement issues and challenges," *IEEE Instrum. Meas. Mag.*, vol. 17, no. 6, pp. 36–42, Dec. 2014.
[53] A. Abur and A. Exposito, *Power System State Estimation (Theory and Implementation)*. New York, NY, USA: Marcel Dekker, 2004.
[54] D. Macii, D. Fontanelli, and G. Barchi, "A distribution system state estimator based on an extended Kalman filter enhanced with a prior evaluation of power injections at unmonitored buses," *Energies*, vol. 13, no. 22, p. 6054, Nov. 2020.
[55] D. Macii, G. Barchi, and D. Petri, "Uncertainty sensitivity analysis of WLS-based grid state estimators," in *Proc. IEEE Int. Workshop Appl. Meas. Power Syst.(AMPS)*, Aachen, Germany, Sep. 2014, pp. 1–6.
[56] D. J. Reid, "Genetic algorithms in constrained optimization," *Math. Comput. Model.*, vol. 23, no. 5, pp. 87–111, Mar. 1996.
[57] W. M. Grady, M. J. Samotyj, and A. H. Noyola, "The application of network objective functions for actively minimizing the impact of voltage harmonics in power systems," *IEEE Trans. Power Del.*, vol. 7, no. 3, pp. 1379–1386, Jul. 1992.
[58] D. Das, D. P. Kothari, and A. Kalam, "Simple and efficient method for load flow solution of radial distribution networks," *Int. J. Electr. Power Energy Syst.*, vol. 17, no. 5, pp. 335–346, Oct. 1995.
[59] H. M. Khodr, F. G. Olsina, P. M. D. O.-D. Jesus, and J. M. Yusta, "Maximum savings approach for location and sizing of capacitors in distribution systems," *Electr. Power Syst. Res.*, vol. 78, no. 7, pp. 1192–1203, Jul. 2008.

[60] K. Deb, S. Agrawal, A. Pratap, and T. Meyarivan, "A fast elitist non-dominated sorting genetic algorithm for multi-objective optimization: NSGA-II," *Lecture Notes in Computer Science (Including Subseries Lecture Notes in Artificial Intelligence and Lecture Notes in Bioinformatics)*, vol. 1917. Berlin, Germany: Springer, 2000, pp. 849–858.
[61] E. Zitzler, L. Thiele, M. Laumanns, C. M. Fonseca, and V. G. da Fonseca, "Performance assessment of multiobjective optimizers: An analysis and review," *IEEE Trans. Evol. Comput.*, vol. 7, no. 2, pp. 117–132, Apr. 2003.
[62] *IEEE/IEC International Standard–Measuring Relays and Protection Equipment—Part 118-1: Synchrophasor for Power Systems–Measurements*, Standard IEC/IEEE 60255-118-1:2018, Dec. 2018, pp. 1–78.
[63] R. D. Zimmerman, C. E. Murillo-Sanchez, and R. J. Thomas, "MATPOWER: Steady-state operations, planning, and analysis tools for power systems research and education," *IEEE Trans. Power Syst.*, vol. 26, no. 1, pp. 12–19, Feb. 2011.
[64] D. Macii, G. Barchi, and L. Schenato, "On the role of phasor measurement units for distribution system state estimation," in *Proc. IEEE Workshop Environ., Energy, Struct. Monitor. Syst.*, Naples, Italy, Sep. 2014, pp. 1–6.
[65] D. Macii, G. Barchi, and D. Moser, "Impact of PMUs on state estimation accuracy in active distribution grids with large PV penetration," in *Proc. IEEE Workshop Environ., Energy, Struct. Monitor. Syst. (EESMS)*, Trento, Italy, Jul. 2015, pp. 72–77.

RICCARDO ANDREONI received the B.S. degree in mechanical engineering from the University of Padua, Italy, in 2017, and the M.S. degree in mechatronics engineering from the University of Trento, Italy, in 2020. His M.S. Thesis is entitled "Multiobjective optimization of the position of phasor measurement units in power systems based on the NSGA II genetic algorithm." He is currently a Process Engineer with Zobele Holding S.p.A., Trento, Italy. His research interests include operations research and genetic algorithms.

DAVID MACII (Senior Member, IEEE) received the M.S. degree in electronics engineering and the Ph.D. degree in information engineering from the University of Perugia, Perugia, Italy, in 2000 and 2003, respectively. He was a Visiting Researcher with the University of Westminster, London, U.K., in 2002. From 2004 to 2005, he was the Advanced Learning and Research Institute, University of Lugano, Lugano, Switzerland. From 2009 to 2010, he was a Fulbright Research Scholar with the Berkeley Wireless Research Center, University of California at Berkeley, Berkeley, CA, USA. He is currently an Associate Professor with the Department of Industrial Engineering University of Trento, Trento, Italy. His research interests include measurement and estimation techniques for a variety of applications, most notably industrial electronics, and power systems. He is the author and coauthor of about 140 papers published in books, scientific journals, and international conference proceedings. Since 2018, he has been an Editor for the journal *Measurement*.

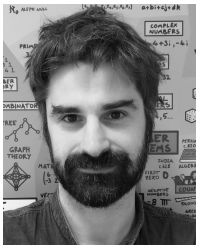

MATTEO BRUNELLI received the Ph.D. degree from Åbo Akademi University, Finland. He spent five years as a Postdoctoral Researcher with the Systems Analysis Laboratory, Aalto University, Finland. He is currently an Associate Professor of mathematical methods for economics with the Department of Industrial Engineering, University of Trento, Italy. His research interests include decision analysis, applied optimization, and mathematical representation of uncertainty.

DARIO PETRI (Fellow, IEEE) received the M.Sc. degree *(summa cum laude)* and the Ph.D. degree in electronics engineering from the University of Padua, Padua, Italy, in 1986 and 1990, respectively. He is currently a Full Professor in measurement science and electronic instrumentation and the Head of the Department of Industrial Engineering, University of Trento, Trento, Italy. During his research career, he has been authored of about 350 papers published in international journals or in proceedings of peer-reviewed international conferences. His research interests include digital signal processing applied to measurement problems, data acquisition systems, and fundamentals of measurement theory. He was the Vice President of the Finance of the IEEE Instrumentation and Measurement Society, from 2013 to 2018, and the Conferences of the IEEE Instrumentation and Measurement Society, from 2011 to 2013. He has been the Chair of the IEEE Smart Cities Initiative in Trento, since 2015. He chaired the Italian Scientific Association of the Researchers working in the area of electrical and electronic measurement, from 2013 to 2016, and the IEEE Italy Section, from 2012 to 2014.